IFSCC 35TH CONGRESS
FRANCE_CANNES 15-18 SEPT 25
THE FUTURE IS SCIENCE
ifscc2025.com

exosome-like nanovesicles derived from *Dunaliella salina* and evaluation of their stability”

Jaehwa Hong [1], Hee Jung Shin [1], Minah Choi [1], Seungmin Han [1], Sangwoo Ruw [2], Eon-Seon Jin [2], Junoh Kim [1,*]

[1] Shinsegae International Inc., Republic of Korea
[2] Department of Life Science, Research Institute for Natural Sciences, Hanyang University, Republic of Korea

1. Introduction

Microalgae are recognized as sustainable biological resources with diverse applications in nutrition, pharmaceuticals, and cosmetics [1,5]. Among them, *D. salina* stands out for its unique physiological traits and its capacity to produce bioactive compounds [13]. This halotolerant green microalga thrives under extreme salinity and intense irradiation, demonstrating remarkable stress tolerance [5], making it ideal for large-scale cultivation and commercial use. One of *D. salina*’s most distinctive features is its ability to accumulate large amounts of β-carotene and other carotenoids, particularly under stress conditions [7]. These pigments function as photoprotective agents, shielding the cells from excessive light and oxidative damage [5,7]. As a result, *D. salina* is widely used as a natural source of antioxidants for nutritional, pharmaceutical, and cosmetic applications [1,15]. In parallel, extracellular vesicles (EVs)—nano-sized, membrane-bound structures secreted by most plant and animal cells—have gained attention for their roles in intercellular communication, transferring proteins, lipids, metabolites, and genetic materials [2,8]. EVs are pivotal in immune regulation, stress responses, and ecological interactions [8]. Although mammalian EVs are well studied, plant- and algal-derived EVs remain relatively underexplored [6]. Plant EVs offer advantages such as lower immunogenicity, sustainability, biocompatibility, and cost-effective scalability [10,14]. Compared to synthetic carriers, plant and algal EVs provide higher yields and simpler extraction processes [2,6]. The integration of microalgae biology and EV technology opens new opportunities for natural nanocarrier development [2,12]. However, algal EVs, including those from *D. salina*, have been less studied [6]. They hold promise as delivery vehicles that combine carrier functionality with intrinsic antioxidant and photoprotective properties [2,12]. Building on this concept, engineered ELs derived from microalgae mimic natural EVs but can be produced under controlled conditions, enabling scalable manufacturing [16]. These ELVs can encapsulate bioactive compounds like carotenoids, maximizing both delivery efficiency and functional benefits [7,12]. In cosmetics, the demand for natural, sustainable, and multifunctional ingredients is rapidly growing [12,14]. EVs and ELVs offer enhanced skin penetration, protect active compounds from degradation, and deliver potential anti-aging, antioxidant, anti-inflammatory, and photoprotective benefits [12,15]. Studies show that EVs loaded with natural ingredients can synergistically improve skin health [12]. Nonetheless, challenges remain for the practical application of microalgae-derived ELVs, including scalable production, physicochemical consistency, storage stability, and formulation compatibility [9,16]. Comprehensive characterization—encompassing size distribution, morphology, zeta potential, and

concentration—is essential for optimizing their applications [10,16]. In this study, we developed a scalable production method for DsELVs using high-pressure homogenization and sequential filtration. The resulting DsELVs demonstrated consistent physicochemical properties and stability under accelerated conditions. Furthermore, surfactant compatibility studies provided insights for formulation development. Carotenoid analysis confirmed the encapsulation of lutein, neoxanthin, violaxanthin, and zeaxanthin, highlighting the multifunctional potential of DsELVs. This research advances natural nanocarrier technology and supports the application of DsELVs in cosmetic, pharmaceutical, and other bioactive formulations.

2. Materials and Methods

2.1. Culture Medium and Culture Conditions

D. salina was cultured in artificial saline water[33] with modifications, containing the following ingredients: Tris–HCl (pH 7.4, 40 mM), KNO_3 (5 mM), $MgCl_2$ (4.5 mM), $MgSO_4$ (0.5 mM), $CaCl_2$ (0.3 mM), K_2HPO_4 (0.1 mM), $FeCl_3$ (2 µM), Na-EDTA (20 µM), H_3BO_3 (50 µM), $MnCl_2$ (10 µM), $ZnSO_4$ (0.8 µM), $CuSO_4$ (0.4 µM), Na_2MoO_4 (2 µM), $NaVO_3$ (1.5 µM), $CoCl_2$ (0.2 µM), and $NaHCO_3$ (25 mM) as an inorganic carbon source. Cultures were grown in a 100 mL volume under continuous white light (85–100 µmol photons m^{-2} s^{-1}) at 25°C. The strain was maintained on an orbital shaker at 140 rpm.

2.2. Preparation by High Pressure Homogenization and Sequential Filtration

D. salina culture was subjected to centrifugation at 4,500 rpm for 3 minutes. After centrifugation, the supernatant was discarded, and the cell pellet was resuspended in purified water to achieve a final cell concentration of 1 × 106 cells/mL. The diluted *D. salina* suspension was processed using a high-pressure homogenizer at a pressure of 2,000 bar, and homogenization was performed for two consecutive cycles to facilitate the formation of nano-sized vesicles. Following homogenization, the resulting suspension was subjected to sequential filtration to remove larger particulates and refine the vesicle population. Filtration was performed in the following order: first through a 2.7 µm Microfiber Glass GF2 filter (CHMLAB, Spain), then a 1.0 µm Microfiber Glass GF4 filter (CHMLAB, Spain), and finally a 0.45 µm PVDF4547A membrane filter (SciLab, Korea). Each filtration step was conducted under gentle vacuµm to minimize vesicle deformation or aggregation. To the final filtrate, a preservative mixture was added to ensure microbial stability during storage. Specifically, 2% (v/v) of 1,2-hexanediol and 0.05% (v/v) of ethylhexylglycerin were incorporated into the vesicle suspension, resulting in a final composition of 97.95% filtered vesicle solution, 2% 1,2-hexanediol, and 0.05% ethylhexylglycerin. The prepared DsELVs samples were then stored at the designated conditions for subsequent analyses.

2.3. Cryo-TEM Analysis

Grids (Lacey/Carbon 200 Mesh, Copper, EMS) were made of hydrophilic surfaces with the glow discharge system (PELCO easiGlow™, Ted Pella). 3 µL of ELVs were added to the grid and blotted for 3 seconds at 100 % humidity and a temperature of 4 °C. Then, the sample was plunge-frozen for vitrification using a Vitrobot Mark IV (Thermo Fisher Scientific, Waltham, USA) in liquid ethane. The samples were analyzed by Glacios (Thermo Fisher Scientific, Waltham, USA) at 200 kV.

2.4. DLS Analysis

The size distribution of ELVs was determined by DLS using a Zetasizer Pro instrument (Malvern, UK). For measurement, each ELV sample was diluted to an appropriate concentration with purified water and transferred into a disposable cuvette (DTS0012, Malvern, UK) prior to analysis. All measurements were conducted at 25°C.

2.5. NTA Analysis

The quantification of ELV particles was performed using a Nanosight NS300 nanoparticle characterization system (Malvern, UK). Prior to analysis, samples were diluted in PBS to an appropriate concentration and introduced into the Blue488 laser chamber via syringe injection. The chamber temperature was maintained at 25°C throughout the measurement.

2.6. Evaluation of Particle Size Stability in the Presence of Surfactants

To evaluate the stability of ELVs with cosmetic surfactants, ELVs solution (5%, v/v), surfactants (0.25%, v/v), and purified water (94.75%, v/v) were mixed. Surfactants tested included PEG-40 Hydrogenated Castor Oil (PEG-40 HCO), PEG-60 Hydrogenated Castor Oil (PEG-6 0 HCO), PPG-13-Decyltetradeceth-24, Polysorbate 20, Polysorbate 60, Polysorbate 80, and Polyglyceryl-10 Laurate. After vortexing, particle size was measured by DLS at 25°C immediately and after 4 weeks of storage at 25°C. Samples were diluted appropriately in purified water before measurement. Stability was assessed by comparing particle size distributions at both time points.

2.7. HPLC Analysis

Pigment analysis was performed using high-performance liquid chromatography (HPLC) following the method described in a previous paper. Pigments were extracted by pipetting the pellet into 0.5 mL of 90% (w/w) acetone. After centrifugation at 13,000 ×g for 2 min, the supernatant was filtered through a 0.2 μm nylon filter. The filtrate was analyzed on a Shimadzu Prominence HPLC system (model LC-20AD) (Shimadzu, Kyoto, Japan), equipped with a Waters Spherisorb S5 ODS2 cartridge column (4.6 × 250 mm) (Waters, MA, USA). HPLC analysis was conducted according to the method described by Park et al.[46] Pigments were identified by retention time and absorption spectra with reference to pigment standards (DHI 14C Centralen, Denmark). The concentrations of individual pigments were determined by HPLC using the same standards.

3. Results

3.1. Characterization of DsELVs

DLS analysis revealed that DsELVs from *D. salina* had a consistent unimodal and narrow size distribution (~125–230 nm), regardless of homogenization passes (1 or 2) or filter pore size (1.0 μm or 0.45 μm), with over 75% of particles within this range. No significant aggregation was observed (Figure 1a). Cryo-TEM confirmed their spherical morphology and distinct bilayer membranes (Figure 1b). Zeta potential values ranged from –25.3 mV to –29.5 mV, indicating strong electrostatic repulsion and good colloidal stability (Figure 1c). NTA showed high and reproducible particle concentrations (5.03×10^9–6.27×10^9 particles/mL) with low variability (≤5×10^8 particles/mL) (Figure 1d).

3.2. Stability Analysis of DsELVs by DLS and NTA

The particle size stability of DsELVs was evaluated by DLS under various storage conditions (5 °C, 25 °C, and 40 °C) over three months. Regardless of filter pore size (1.0 µm or 0.45 µm) or the number of high-pressure homogenization passes (1 or 2), DsELVs maintained a consistent size distribution. Initial mean diameters ranged from approximately 187 nm to 219 nm and remained stable with only minor fluctuations after three months: 167–193 nm at 5 °C, 177–195 nm at 25 °C, and 173–180 nm at 40 °C. (Figure 2a). Zeta potential measurements showed consistently high absolute negative charges (–25.3 mV to –34.1 mV) across all conditions, supporting excellent colloidal stability (Figure 2b). NTA further confirmed that particle concentrations remained high (approximately 5.0 × 10⁹ to 6.3 × 10⁹ particles/mL) with minimal variation, indicating sustained structural integrity over time (Figure 2c). Overall, these results demonstrate that DsELVs maintain excellent stability in size, surface charge, and concentration under diverse storage conditions, highlighting their potential for cosmetic and pharmaceutical applications.

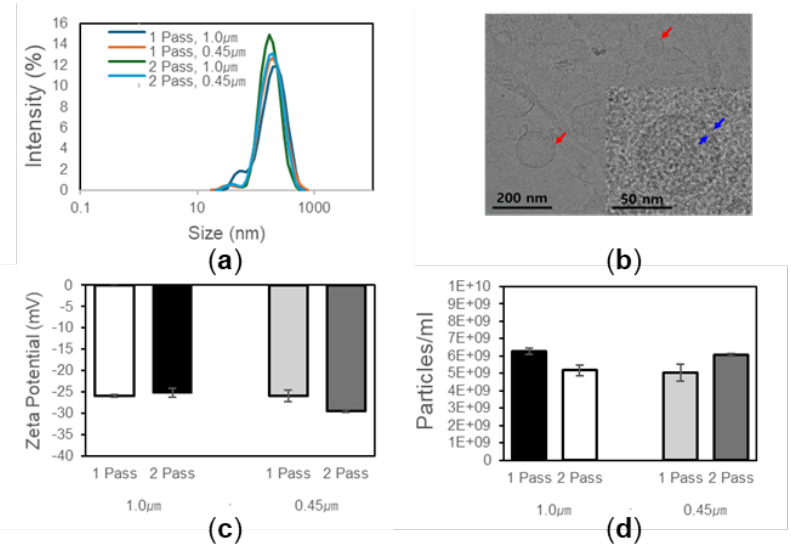

Figure 1. Characterization of DsELVs: (a) Particle size distribution measured by DLS under various homogenization and filtration conditions; (b) Representative Cryo-TEM image (c) Zeta potential values measured by DLS; (d) Particle concentration determined by NTA

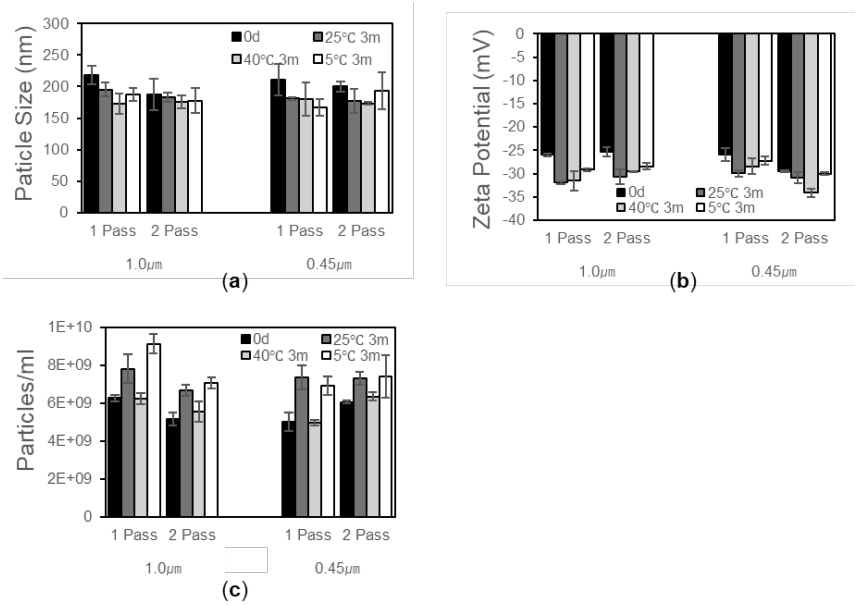

Figure 2. Stability analysis of DsELVs under various storage conditions: (a) Particle size distribution measured by DLS; (b) Zeta potential values measured by DLS; (C) Particle concentration determined by NTA

3.3. Particle Size Stability of DsELVs in Various Surfactant Solutions

The particle size stability of DsELVs in the presence of various surfactants was evaluated by DLS immediately after mixing (day 0) and after 4 weeks of storage at 25 °C (Table 1). Across all tested surfactants—including PEG-40 and PEG-60 Hydrogenated Castor Oil, PPG-13-Decyltetradeceth-24, Polysorbates 20, 60, and 80, and Polyglyceryl-10 Laurate—DsELVs maintained a predominant nanometer-sized population (typically 150–230 nm) with minimal changes in mean diameter and area percentage over time. In all formulations, the main particle population remained stable with negligible secondary populations and no signs of aggregation. These results indicate that the tested surfactants do not adversely affect the size distribution or colloidal stability of DsELVs. Overall, DsELVs retained their characteristic nanoscale vesicular structure and exhibited excellent compatibility with a wide range of surfactants, supporting their potential incorporation into cosmetic formulations.

3.4. Retention of D. salina-Derived Carotenoids in DsELVs

Carotenoid analysis of DsELVs prepared by two cycles of high-pressure homogenization and 0.45 μm membrane filtration revealed four major components: lutein, neoxanthin, violaxanthin, and zeaxanthin (Table 2). Lutein was the most abundant (0.250 μg/L), followed by neoxanthin (0.036 μg/L), violaxanthin (0.024 μg/L), and zeaxanthin (0.016 μg/L). These results confirm that DsELVs retain bioactive carotenoids derived from D. salina, with lutein as the predominant compound. The presence of these functional molecules may contribute to the potential cosmetic and therapeutic value of DsELVs.

Table 1. Effect of Surfactants on the Particle Size Stability of DsELVs

No.	Sample Name (Day(s) post-mixing)	Size (Area%)
1	DsELVs (0d)	181.2 nm (91.13%), 35.03 (8.869%)
	DsELVs (4w)	204.7 nm (92.01%), 34.25 (7.989%)
2	PEG-40 HCO (0d)	15.76 nm (100%)
	PEG-40 HCO + DsELVs (0d)	170.1 (79.68%), 15.96 nm (20.32%)
	PEG-40 HCO + DsELVs (4w)	162.9 (74.66%), 15.97 nm (22.68%)
3	PEG-60 HCO (0d)	16.17 nm (100%)
	PEG-60 HCO + DsELVs (0d)	233.7 (86.85%), 15.55 nm (13.15%)
	PEG-60 HCO + DsELVs (4w)	195.2 (81.88%), 15.48 nm (18.12%)
4	PPG-13-Decyltetradeceth-24	15.51 nm (100%)
	PPG-13-Decyltetradeceth-24 + DsELVs (0d)	190.7 (79.21%), 16.5 nm (20.79%)
	PPG-13-Decyltetradeceth-24 + DsELVs (4w)	160.3 (74.96%), 15.98 nm (25.04%)
5	Polysorbate 20	9.55 nm (100%)
	Polysorbate 20 + DsELVs (0d)	152.6 (92.1%), 15.51 nm (7.45%)
	Polysorbate 20 + DsELVs (4w)	210.5 (89.75%), 23.12 nm (8.6%)
6	Polysorbate 60	11.94 nm (100%)
	Polysorbate 60 + DsELVs (0d)	158.6 (86.97%), 13.57 nm (13.33%)
	Polysorbate 60 + DsELVs (4w)	148.5 (83.99%), 13.17 nm (16%)
7	Polysorbate 80	11.69 nm (100%)
	Polysorbate 80 + DsELVs (0d)	159.5 (86.98%), 12.94 nm (13.02%)
	Polysorbate 80 + DsELVs (4w)	165.8 (83.73%), 13.1 nm (14.18%)
8	Polyglyceryl-10 Laurate	12.22 nm (100%)
	Polyglyceryl-10 Laurate + DsELVs (0d)	298.3 (56.46%), 49.75 nm (43.44%)
	Polyglyceryl-10 Laurate + DsELVs (4w)	160.3 (74.96%), 15.98 nm (25.04%)

Table 2. Carotenoid Content Analysis of DsELVs.

Carotenoid	Content (μg/L)
Neoxanthin	0.036
Violaxanthin	0.024
Lutein	0.250
Zeaxanthin	0.016

4. Discussion

DsELVs exhibited a uniform size distribution (125–230 nm), spherical morphology with intact bilayer membranes, a negative surface charge (–25.3 to –29.5 mV), and high particle concentrations (5.03–6.27 × 10^9 particles/mL). These properties resemble those of natural mammalian exosomes (30–150 nm), with the larger size likely due to differences in membrane composition and production process. However, this size range remains ideal for dermal delivery, as nanoparticles between 100–300 nm can penetrate hair follicles and reach deeper skin layers [18, 19]. The negative zeta potential values ensure electrostatic repulsion between particles, contributing to colloidal stability. Similar surface charge characteristics have been reported in plant-derived nanovesicles, with absolute zeta potential values exceeding ±25 mV providing adequate electrostatic stabilization [20, 21]. Furthermore, the high

particle concentrations indicate an efficient and scalable production process, overcoming the limitations of ultracentrifugation commonly used for plant-derived extracellular vesicles [22].

DsELVs displayed remarkable stability under different storage conditions (5°C, 25°C, and 40°C) for up to three months. This exceeds the stability of conventional liposomal systems, which often require refrigeration or lyophilization [23]. Minimal changes in particle size, zeta potential, and concentration during storage suggest that the natural composition of DsELVs, rich in lipids and carotenoids, contributes to their resilience [24, 25]. As *D. salina* naturally thrives in high-salinity environments with fluctuating temperatures, this may explain the enhanced stability of DsELVs, similar to other extremophile-derived lipid systems [26]. The thermostability of DsELVs is especially advantageous for cosmetic formulations, as many nanocarriers degrade or aggregate at elevated temperatures. This feature makes DsELVs suitable for real-world cosmetic applications.

DsELVs demonstrated excellent compatibility with various cosmetic surfactants, maintaining their integrity and size distribution over four weeks. Surfactants are essential in cosmetic formulations for solubilization, emulsification, and enhancing ingredient delivery [27]. Unlike conventional phospholipid vesicles, which are destabilized by surfactants, DsELVs remained stable due to the unique composition of microalgal membranes, which contain glycolipids and sterols resistant to surfactant-induced disruption [29, 30]. The stability of DsELVs with PEG-modified surfactants and polysorbates suggests their broad compatibility with different cosmetic formulations, from serums to emulsions [31].

The physicochemical properties and stability of DsELVs make them promising for cosmetic and pharmaceutical applications. The nano-sized dimensions (125–230 nm) facilitate effective skin interaction and stability in formulations [32]. DsELVs inherently contain carotenoids such as β-carotene, which offer antioxidant and photoprotective benefits [34]. Plant-derived extracellular vesicles retain bioactive compounds, providing additional skin benefits beyond delivery [35, 36]. With the growing demand for natural, sustainable cosmetic ingredients, DsELVs could appeal to consumers seeking eco-friendly products [37].

Compared to conventional liposomes, DsELVs show superior stability under accelerated conditions. While liposomes often require cholesterol or special storage conditions, DsELVs retained consistent properties for up to three months, even at elevated temperatures [23, 38]. When compared to other plant-derived nanovesicles, DsELVs demonstrate comparable or superior stability, particularly in terms of thermostability [39, 40]. The high-pressure homogenization method used here offers advantages over more complex extraction procedures like ultracentrifugation, making it more suitable for large-scale production [41].

Despite these promising results, further studies are needed to address a few limitations. First, the chemical stability of membrane components and encapsulated compounds should be evaluated, as lipid oxidation can affect both stability and bioactivity [34]. Second, the biological interactions of DsELVs with skin models, such as reconstructed human epidermis or Franz diffusion cells, should be explored to assess dermal delivery potential [32, 42]. Investigations into cellular uptake mechanisms would also help understand how DsELVs interact with skin cells at the molecular level [43]. Third, while compatibility with various surfactants was demonstrated, further studies are necessary to assess interactions with other cosmetic ingredients like preservatives and active compounds. Finally, encapsulation efficiency for various actives should be evaluated to determine the practical utility of DsELVs as delivery systems [44, 45].

5. Conclusion

Our study demonstrates that DsELVs possess excellent physicochemical properties, strong stability under various storage conditions, and compatibility with cosmetic surfactants. These characteristics make DsELVs promising natural nanocarriers for cosmetic and pharmaceutical applications. Furthermore, the sustainable production of these bio-derived vesicles aligns with the increasing consumer demand for natural, eco-friendly ingredients. Future research focusing on their biological interactions, encapsulation capabilities, and formulation optimization will be essential to fully unlock their potential in commercial applications.

References

1. Alagawany M, et al. Dietary supplementation with Dunaliella salina micro-alga promotes quail growth by altering lipid profile and immunity. Poultry Science. 2024;103(5):103591.
2. Kuruvinashetti K, Pakkiriswami S, Packirisamy M. Algal extracellular vesicles for therapeutic applications. 2020 IEEE 20th International Conference on Nanotechnology (IEEE-NANO). 2020:366-369.
3. Amer MS. Dunaliella salina-silver nanoparticle biosynthesis. Semantic Scholar. 2023.
4. Pranav A. Formulation and evaluation of alginate-based ocular inserts of fexofenadine hydrochloride. Hypertension, Fundamental & Biomedical Science. 2023;3(2 Suppl):177-186.
5. Shantkriti S, et al. Biosynthesis of silver nanoparticles using Dunaliella salina and its antibacterial applications. Appl Surf Sci Adv. 2023;13:100377.
6. Li-Hammed MA, et al. Comparative biochemical profiling and industrial application potentials of Dunaliella salina and Spirulina platensis.
7. Guermazi W, et al. Physiological and biochemical responses in microalgae Dunaliella salina, Cylindrotheca closterium and Phormidium versicolor NCC466 exposed to high salinity and irradiation. Life. 2023;13(2):313.
8. Xu Y, Harvey PJ. Mitosis inhibitors induce massive accumulation of phytoene in the microalga Dunaliella salina. Mar Drugs. 2021;19(11):595.
9. Dai JL, et al. Dual roles of two malic enzymes in lipid biosynthesis and salt stress response in Dunaliella salina. J Agric Food Chem. 2023;71(45):17067-17079.
10. Hermawan J, et al. Increasing β-carotene content of phytoplankton Dunaliella salina using different salinity media. IOP Conf Ser Earth Environ Sci. 2018;137.
11. Liang MH, et al. Roles of two phytoene synthases and orange protein in carotenoid metabolism of the β-carotene-accumulating Dunaliella salina. Microbiol Spectr. 2023;11(3):e00069-23.
12. Çelebi H, et al. Use of Dunaliella salina in environmental applications. Proceedings of 1st International Electronic Conference on Biological Diversity, Ecology and Evolution. 2021;9411.
13. Konar N, et al. Spray-drying optimization for Dunaliella salina and Porphyridium cruentum biomass. Drying Technol. 2023;41(15):2371-2384.
14. Song J, et al. Effect of Dunaliella salina on myocardial ischemia-reperfusion injury through KEAP1/NRF2 pathway activation and JAK2/STAT3 pathway inhibition. Gene Protein Dis. 2023;2(2):387.
15. Katz A, Kaback HR, Avron M. Na+/H+ antiport in isolated plasma membrane vesicles from the halotolerant alga Dunaliella salina. FEBS Lett. 1986;202(1):141-144.
16. Vlassov AV, et al. Exosome biology and diagnostic and therapeutic potential of exosomal proteins and RNA. Biochim Biophys Acta Gen Subj. 2012;1820(7):940-948.

17. Lademann J, et al. Penetration of titanium dioxide microparticles in a sunscreen formulation into hair follicles after application to the skin. Eur J Pharm Biopharm. 2007;66(2):159-164.
18. Prow TW, et al. Nanoparticles and microparticles for skin drug delivery. Adv Drug Deliv Rev. 2011;63(6):470-491.
19. Woith E, et al. Plant extracellular vesicles-purification and visualization using AFM and TEM. Int J Mol Sci. 2019;20(2):357.
20. Bhattacharjee S, et al. DLS and zeta potential–what they are and what they are not? J Control Release. 2016;235:337-351.
21. Raimondo S, et al. Citrus limon-derived nanovesicles inhibit cancer cell proliferation and suppress CML xenograft growth by inducing TRAIL-mediated cell death. Oncotarget. 2015;6(23):19514-19527.
22. Briuglia ML, et al. Influence of cholesterol on liposome stability and on in vitro drug release. Drug Deliv Transl Res. 2015;5:231-242.
23. Oren A. 100 years of Dunaliella research: 1905–2005. Saline Syst. 2005;1:2.
24. Parmar A, et al. Cyanobacteria and microalgae: a positive prospect for biofuels. Bioresour Technol. 2011;102(22):10163-10172.
25. Çelik B, et al. Design, characterization and in vitro evaluation of coenzyme Q10 loaded liposomes for oral drug delivery. Int J Nanomedicine. 2017;12:4869-4878.
26. Tadros TF. Applied Surfactants: Principles and Applications. Wiley-VCH; 2005.
27. López O, et al. Solubilization of phospholipid liposomes by sodium dodecyl sulfate: effect of vesicle size and lipid composition. Arch Biochem Biophys. 1999;367(1):153-160.
28. Nuutila AM, et al. Production of eicosapentaenoic acid by Porphyridium cruentum (Heterokontophyta, Rhodophyta) as a function of salinity and nitrate concentration. J Biotechnol. 1997;55(1):55-63.
29. Hölzl G, Dörmann P. Structure and function of glycoglycerolipids in plants and bacteria. Prog Lipid Res. 2007;46(3–4):225-243.
30. Fiume MZ, et al. Safety assessment of polyethylene glycol (PEG) compounds for use in cosmetics. Int J Toxicol. 2012;31(Suppl 2):138S-160S.
31. Cevc G, Gebauer G. Hydration-driven transport of deformable vesicles through fine pores and the skin barrier. J Control Release. 2010;141(3):277-292.
32. Pick U. The plant vacuole: a multifunctional compartment. Plant Physiol. 1986;85(1):195-198.
33. Lamers PP, et al. Carotenoid synthesis in Dunaliella salina: biochemical pathways and metabolic engineering. Trends Biotechnol. 2008;26(11):631-638.
34. Mu J, et al. Exosome-like nanoparticles from edible plants carrying microRNA regulate expression of mouse genes. Mol Nutr Food Res. 2014;58(7):1561-1573.
35. Dad HA, et al. Plant exosome-like nanoparticles: emerging therapeutics and drug delivery nanoplatforms. Mol Ther. 2021;29(1):13-31.
36. Grand View Research. Organic personal care market size, share & trends analysis report by product, by region, and segment forecasts, 2020–2027. Grand View Research; 2020.
37. Paliwal SR, et al. Design and development of pH-sensitive liposomes for oral delivery of docetaxel: in vitro and in vivo evaluation. Drug Deliv. 2015;22(2):231-242.
38. Zhang M, et al. Edible ginger-derived nanoparticles: a novel therapeutic approach for the prevention and treatment of inflammatory bowel disease and cancer. Biomaterials. 2016;101:321-340.
39. Ju S, et al. Grape exosome-like nanoparticles induce intestinal stem cells and protect mice from DSS-induced colitis. Mol Ther. 2013;21(7):1345-1357.

40. Akuma P, et al. Potential applications of plant-derived extracellular vesicles as natural bioactive nanocarriers: a review. Front Sustain Food Syst. 2019;3:23.
41. Chaudhary H, et al. Development and evaluation of olanzapine-loaded nano-transfersomes for transdermal delivery. Int J Pharm. 2013;454(1):367-380.
42. Rancan F, et al. Investigation of the influence of nano-sized silica particles on dermal penetration using confocal and multiphoton microscopy. ACS Nano. 2012;6(8):6829-6843.
43. Kong M, et al. Hyaluronic acid-decorated niosome as a tumor-targeted nanocarrier for efficient anticancer drug delivery. Carbohydr Polym. 2013;94(1):634-644.
44. Tran N, et al. Cytotoxicity of monoolein–capric acid nanoparticles in HEp-2 and HepG2 cell lines. RSC Adv. 2015;5(34):26785-26795.
45. Kim M, et al. Photoadaptation of Dunaliella salina under different salinity conditions. Algae. 2015;30:129-139.